

Global phase diagram of bilayer quantum Hall ferromagnets

M. Abolfath^{1,2}, L. Radzihovsky³, and A.H. MacDonald²

¹*Department of Physics and Astronomy, University of Oklahoma, Norman, OK 73019*

²*Department of Physics, University of Texas, Austin, TX 78712*

³*Department of Physics, University of Colorado, Boulder, CO 80309*

(October 28, 2018)

We present a microscopic study of the interlayer spacing d versus in-plane magnetic field B_{\parallel} phase diagram for bilayer quantum Hall (QH) pseudo-ferromagnets. In addition to the interlayer charge balanced commensurate and incommensurate states analyzed previously, we address the corresponding interlayer charge unbalanced “canted” QH states. We predict a large anomaly in the bilayer capacitance at the canting transition and the formation of dipole stripe domains with periods exceeding 1 micron in the canted state.

PACS: 73.20.Dx, 11.15.-q, 14.80.Hv, 73.20.Mf

There now exists considerable experimental [1–5] and theoretical [6–10] evidence for interlayer phase coherent states in bilayer quantum Hall (QH) systems at total Landau level filling fraction $\nu_T = 1$. The ground state in these systems can be regarded as an easy-plane ferromagnet [9], as a condensate of electrons in one layer and holes in the Landau level of the other layer [11], or as a superfluid of Chern-Simons composite bosons [8]. The competition between tunneling energy, which pins the interlayer phase, and Coulomb interaction energy, which favors interlayer phase rigidity, yields a rich phenomenology. This is especially true when an in-plane magnetic field component B_{\parallel} , that favors the development of Aharonov-Bohm (AB) phases, is present. The nature of the ground state is dependent on the separation d between layers, on the strength of interlayer tunneling, which is conventionally parameterized by the splitting Δ_{SAS} between symmetric and antisymmetric bilayer single-particle states, and for $\Delta_{SAS} \neq 0$ on B_{\parallel} .

In this Letter we present a microscopic theory of the $d - B_{\parallel}$ phase diagram, allowing for the *spontaneously* interlayer charge unbalanced “canted” commensurate (C) and incommensurate (I) QH states proposed recently by one of us [13], in addition to the corresponding charge balanced “planar” QH states. [9] Our main results are summarized by the phase diagram of Fig.1, where five different phases occur. In the pseudospin ferromagnet language, the effect of tunneling is to add to the Hamiltonian an in-plane Zeeman *pseudo*-field, which winds uniformly in space along the \hat{x} axis at rate $Q = (B_{\parallel}/B_{\perp})(d/\ell^2)$ for a field in the \hat{y} direction. Here the magnetic length ℓ is related to the perpendicular field by $2\pi\ell^2 B_{\perp} = hc/e$. In the *planar* charge balanced commensurate (CP) QH state, the pseudospin magnetization faithfully follows the winding pseudo-field and its azimuthal angle is given by $\phi(\mathbf{r}) = Qx$. For sufficiently large Q , however, the cost in exchange energy of this variation becomes too large and phase-slip solitons are nucleated, leading to a incom-

mensurate planar (IP) QH ground state, with the CP-IP transition in the universality class of the well-studied C-I transition [15]. Within the Hartree-Fock (HF) theory we employ, the large d instability, previously studied only at $Q = 0$, is to a Wigner crystal state of the bilayer system [6,7]. It has been argued previously [7] that quantum melting of this crystal leads to a state which does not have broken translational symmetry but, like the Wigner crystal, is compressible, does not exhibit a QH effect, and is not distinguished by any symmetry from the state with uncorrelated $\nu = 1/2$ layers that is expected at very large d . We have followed [16] that suggestion here by labeling this region “No-QHE”. Our work focuses on the small d instabilities of the planar QH pseudospin ferromagnets.

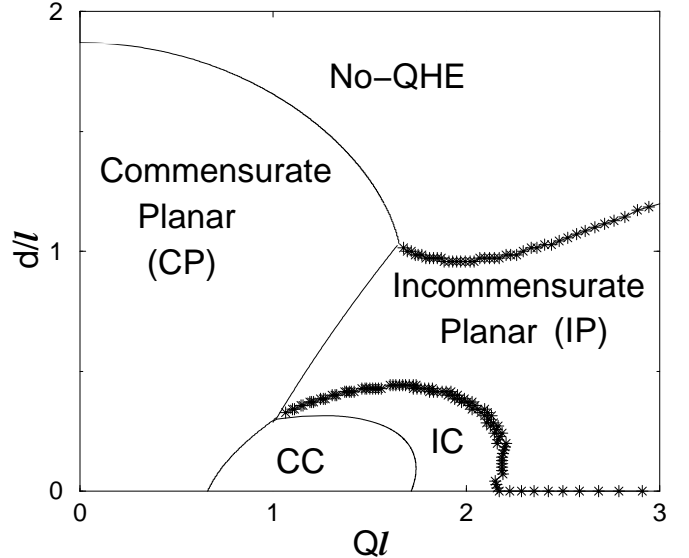


FIG. 1. Phase diagram illustrating the commensurate planar (CP), incommensurate planar (IP), commensurate canted (CC), and incommensurate canted (IC) QH states, for $\Delta_{SAS} = 0.126e^2/\epsilon\ell$. For smaller Δ_{SAS} , canted and incommensurate states shift to smaller Q . The nature of the compressible “No-QHE” state cannot be established on the basis of HF theory.

At small d and intermediate in-plane fields, we find that B_{\parallel} drives the easy-plane XY anisotropy [12] of these quantum Hall ferromagnets through zero, leading to a continuous Ising-like *reentrant* quantum transitions from the charge *balanced* CP and IP QH states to the corresponding commensurate (CC) and incommensurate (IC) interlayer charge *unbalanced* canted QH phases, recently predicted by one of us [13]. Our $d - B_{\parallel}$ phase diagram (Fig.1) was constructed by considering a set of single-Slater-determinant variational wavefunctions which allow translational symmetry to be broken in one direction:

$$|\Psi[\hat{\mathbf{m}}_X]\rangle = \prod_X (u_X c_{T,X}^{\dagger} + v_X c_{B,X}^{\dagger})|0\rangle, \quad (1)$$

$$E_{HF}[\hat{\mathbf{m}}_X] = -\frac{1}{2}\Delta_{SAS} \sum_X \sin\theta_X \cos(\phi_X - QX) + \frac{1}{4L_y} \sum_{X,X'} [2H(X - X') - F_S(X - X')] \cos\theta_X \cos\theta_{X'} \\ - \frac{1}{4L_y} \sum_{X,X'} F_D(X - X') \sin\theta_X \sin\theta_{X'} \cos(\phi_X - \phi_{X'}), \quad (2)$$

where $\Delta_{SAS} = \Delta_{SAS}^{(0)} e^{-Q^2\ell^2/4}$ varies weakly with in-plane field, and we have assumed a presence of a fixed neutralizing background of positive charge. In the above, the terms proportional to $H(X)$ arise from Hartree (electrostatic) contributions to the energy functional, while those proportional to $F_S(X)$ and $F_D(X)$ originate from Fock (exchange) interactions between electrons in same and different layers respectively. The first term in $E_{HF}[\hat{\mathbf{m}}_X]$ is due to interlayer tunneling and incorporates the AB phases in the factor $\cos(\phi_X - QX)$. For a model with arbitrarily narrow two-dimensional electron layers

$$H(X) = \int \frac{dq}{2\pi} \frac{2\pi e^2(1 - e^{-qd})}{2q} e^{iqX} e^{-q^2\ell^2/2}, \quad (3a)$$

$$\frac{\sin(\phi_X)}{\cos(\phi_X)} = \frac{\Delta_{SAS} \sin(QX) + \frac{1}{L_y} \sum_{X'} F_D(X - X') \sin(\theta_{X'}) \sin(\phi_{X'})}{\Delta_{SAS} \cos(QX) + \frac{1}{L_y} \sum_{X'} F_D(X - X') \sin(\theta_{X'}) \cos(\phi_{X'})}, \quad (4a)$$

$$\frac{\cos(\theta_X)}{\sin(\theta_X)} = \frac{\frac{1}{L_y} \sum_{X'} \cos(\theta_{X'}) [F_S(X - X') - 2H(X - X')]}{\Delta_{SAS} \cos(\phi_X - QX) + \frac{1}{L_y} \sum_{X'} \sin(\theta_{X'}) F_D(X - X') \cos(\phi_X - \phi_{X'})}. \quad (4b)$$

Eqs.4a,4b follow from the minimization of $E_{HF}[\hat{\mathbf{m}}_X]$ with respect to ϕ_X and θ_X , respectively. The numerator and denominator on the right hand side of Eq. 4a are the \hat{x} and \hat{y} components of the pseudospin Zeeman effective fields seen by the Hartree-Fock quasiparticles, which include contributions from interlayer exchange interactions. Note that the exchange local pseudo-field decreases when ϕ_X is not constant. Equation 4b expresses the property that in the HF ground state the pseudospin is aligned at each X along the direction of the pseudospin Zeeman effective field. For example, the com-

where $c_{T,X}^{\dagger}$ and $c_{B,X}^{\dagger}$ create electrons in top (T) and bottom (B) layers respectively, X is a Landau gauge guiding center label in the lowest Landau level, and the pseudospin magnetization $\hat{\mathbf{m}}_X = (\sin\theta_X \cos\phi_X, \sin\theta_X \sin\phi_X, \cos\theta_X)$ at label X is the coherent state label of the spinor (u_X, v_X) , *i.e.* $(u_X, v_X) = (\cos[\theta_X/2], \sin[\theta_X/2] \exp[i\phi_X])$. In these wavefunctions ϕ_X is the local pseudospin phase coherence angle and θ_X is the local polar angle that specifies the magnitude of the charge imbalance between top and bottom layers. Taking the expectation value of the microscopic Hamiltonian \mathcal{H} , this variational wavefunction leads to the microscopic energy functional $E_{HF}[\hat{\mathbf{m}}_X] = \langle \Psi[\hat{\mathbf{m}}_X] | \mathcal{H} | \Psi[\hat{\mathbf{m}}_X] \rangle$

$$F_C(X) = e^{-X^2/2\ell^2} \int \frac{dq}{2\pi} V_C(q, X/\ell^2) e^{-q^2\ell^2/2}, \quad (3b)$$

where $V_C(q_x, q_y) = 2\pi e^2/q$ and $2\pi e^2 \exp(-qd)/q$ for $C = S$ and $C = D$ respectively. Note that the exchange integral drops rapidly with orbit center separation, while the electrostatic integral falls only as X^{-2} at large X , corresponding to interactions between lines of interlayer charge imbalance electric dipoles.

The states we discuss are all extrema of this energy functional and therefore have pseudospin configurations that satisfy the following two equations:

mensurate planar CP state ($\phi_X = QX$ and $\sin(\theta_X) \equiv 1$) solves these equations with a Zeeman pseudospin field $\Delta_{SAS} + \tilde{F}_D(Q)$ lying in the xy-plane (with Fourier transform convention, $\tilde{f}(p) = \frac{1}{L_y} \sum_X f(X) \exp(-ipX)$). Because the same layer exchange energy normally dominates the electrostatic energy, the \hat{z} component of the effective pseudo-field tends to have the same sign as the \hat{z} component of the pseudospin, enabling the canted configurations we will discuss shortly.

The CP and IP ground states are stable against canting if all eigenvalues of the following matrix are positive:

$$K_{zz}(X, X') \equiv \frac{1}{2\pi} \left. \frac{\delta^2 E_{HF}}{\delta m_X^z \delta m_{X'}^z} \right|_{m_z=0} = \frac{1}{4\pi L_y} [2H(X - X') - F_S(X - X')]$$

$$+ \frac{1}{4\pi} \delta_{X,X'} \left[\Delta_{SAS} \cos(\phi_X - QX) + \frac{1}{L_y} \sum_{X'} F_D(X - X') \cos(\phi_X - \phi_{X'}) \right]. \quad (5)$$

In the CP state, translational invariance simplifies the evaluation of the eigenvalue spectrum of $K_{zz}(X, X')$ which has plane waves $\exp(ipX)$ eigenfunctions with eigenvalues $\tilde{K}_{zz}(p) = [\Delta_{SAS} + \tilde{F}_D(Q) + 2\tilde{H}(p) - \tilde{F}_S(p)]/(4\pi)$. An important feature of $\tilde{K}_{zz}(p)$ is the non-analytic linear decrease in $\tilde{H}(p) = (e^2 d/2\ell^2)(1 - pd/2 + p^2(d^2 - 3\ell^2)/6 + \dots)$ at small p , which originates from the slow X^{-2} fall off in the (anti-ferroelectric) dipole electrostatic interactions. One consequence is that the minimum in $\tilde{K}_{zz}(p)$ always occurs at a finite $p = p_c^*$, with $p_c^* \propto d^2$ at small d , (see the inset (a) of Fig.2) leading to a minimum at finite p . For a sufficiently large value of d , $K^* \equiv \tilde{K}_{zz}(p^*)$ is negative even at $Q = 0$; this critical value of d is associated with the onset of the “No-QHE” compressible regime at $Q = 0$. For finite small Q , $\tilde{F}_D(Q) = \tilde{F}_D(0) - 4\pi\rho_s(Q\ell)^2 + \dots$ decreases, thereby expanding the “No QHE” regime quadratically with the applied in-plane field B_{\parallel} , as illustrated in Fig.1.

The physics of the small d part of the phase diagram is different. The minimum of $\tilde{K}_{zz}(p)$ (K^*) occurs at a finite, but much smaller value of p , and decreases with Q , crossing zero before the incommensurate state boundary is reached as illustrated in Fig. 1. The instability is associated with a change in sign of the pseudospin anisotropy energy and is closely analogous to a transition in which the easy axis of a thin-film ferromagnet changes from in-plane to perpendicular-to-plane, forcing the formation of stripe domains [14]. In the quantum Hall case it is *electric* rather than *magnetic* dipole interactions that force the transition to occur at finite wavevector. The CP-CC phase boundary is defined by $K^*(d, Q) = 0$ curve ($d(Q) \approx (8\pi\rho_s\ell^4/e^2)(Q^2 - \xi^{-2})$, rising linearly above the $d = 0$ critical value $Q_{CP-CC} = \xi^{-2}$) as illustrated in Fig. 1. As indicated there, the CP-CC canting instability is preempted at intermediate values of d and Q by the CP-IP commensurate-incommensurate transition, which for small Δ_{SAS} takes place at a small value of $Q = Q_{CP-IP} = 4/(\pi\xi)$, determined by the condition of vanishing soliton energy, with $\xi = \sqrt{4\pi\ell^2\rho_s/\Delta_{SAS}}$ the width of an isolated phase slip soliton in the incommensurate state [15]. Within the HF approximation Q_{CP-CC}/Q_{CP-IP} approaches $\pi/4$ as $d \rightarrow 0$. At finite values of Δ_{SAS} , the CP-IP phase transition is located by extrema of the Hartree-Fock energy functional for which $\tilde{\phi}_X \equiv \phi_X - QX$ is periodic (modulo 2π), at a Q for which the period extrapolates to infinity.

Because of its inhomogeneous nature, locating the canting instability of the IP state is significantly more involved, but conceptually similar to the analysis of the homogeneous CP state discussed above. We first solve the mean-field equations for the IP extremum of the energy

functional, explicitly seeking a self-consistent solution for $\tilde{\phi}_X$ with period a . This minimization is performed numerically for a finite value of L_y so that the number of distinct guiding centers per soliton $N_g = aL_y/(2\pi\ell^2)$ is finite.

The stability limit of this planar soliton lattice QH state is marked by the appearance of a zero eigenvalue in a corresponding $K_{zz}(X, X')$ matrix, which must be computed numerically. In analogy with the CP-CC transition, here the transition is between *planar* (charge-balanced) IP and *canted* (charge-imbalanced) IC phases, both of which are incommensurate QH states, with IC state located on the small d side of this phase boundary, as illustrated in Fig. 1. Some features of these non-trivial numerical results can be understood on the basis of qualitative considerations. [15] For large Q , the AB phases are so unfavorable for interlayer correlations that the ground state approaches a simple state in which tunneling between the layers is ignored completely and ϕ_X approaches a constant to minimize the interaction energy, *i.e.*, $\tilde{\phi}_X = QX$. In this limit the canting stabilities must be the same as those of bilayer systems with $\Delta_{SAS} = 0$. Consequently, as illustrated in Fig. 1 we find that the canting transition is *reentrant* [13], and for large in-plane fields only a single instability to a “No-QHE” state exists, with the critical value of d universally smaller than that for the $Q = 0$ case. The evolution of this IP-IC phase boundary with parallel field is calculated here for the first time, and it would be interesting to test experimentally. In the remainder of the paper we concentrate on the properties of the novel *canted* QH states, CC and IC, at small d , which we expect to be reliably rendered by the Hartree-Fock microscopic theory.

Canted QH phases are distinguished from their planar counterparts by a finite z-component of the pseudo-spin magnetization order parameter, m_z , which measures the interlayer charge imbalance $n_T - n_B = m_z/(2\pi\ell^2)$, that spontaneously develops inside canted states. As discussed above, because the canting instability is at a finite wavevector $p_c^*(d)$, for finite d the order parameter m_X^z is staggered with period $2\pi/p_c^*$. However, in the limit of small $d \ll \ell$, such that $p_c^* \rightarrow 0$ (or looking at scales smaller than $2\pi/p_c^*$), m_X^z is nearly uniform and, as in the magnetic case, it is often a good approximation to ignore the stripe domain structure and look at the $p = 0$ (uniform θ_X) extrema of the energy functional. Eq.4b then leads to nonzero $m_z(d, B_{\parallel}) = \sqrt{1 - \sin^2\theta}$, with $\sin\theta = \Delta_{SAS}/[\tilde{F}_S(0) - 2\tilde{H}(0) - \tilde{F}_D(Q)]$, which therefore predicts the expected mean-field square-root growth of the canting order parameter (Fig.2, inset (b)) inside the CC phase upon crossing the CP-CC phase bound-

ary in any direction. Inside the CC state, Eq.4a predicts the quasi-particle gap (measured through the activated behavior of the longitudinal resistivity) to be $\Delta_{QH} = \Delta_{SAS} + \tilde{F}_D(Q)\sqrt{1 - m_z^2(d, B_{\parallel})}$, reduced relative to that of the CP state.

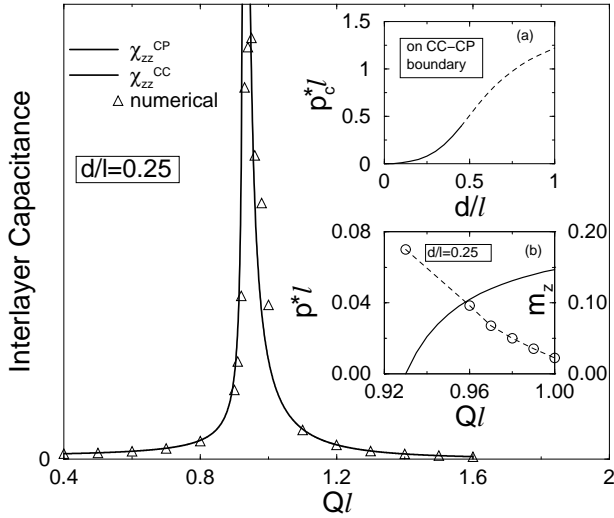


FIG. 2. Bilayer capacitance across CP-CC phase boundary, with peak's height set by wavevector p_c^* (inset (a)) of pseudo-magnetization $m_z(X)$ that spontaneously develops at the transition. Inset (b) shows the increasing lowest harmonic amplitude of $m_z(X)$ and the corresponding wavevector $p^*(Q)$ that decreases inside the CC phase.

We are now in the position to calculate the phase boundary for the CC-IC transition. Since the effect of canting on the soliton physics is to reduce the one-particle tunneling energy by a factor of $\sin\theta$ and the interlayer exchange interaction by a factor of $\sin^2\theta$, standard analysis [15] leads to the phase boundary $Q_{CC-IC}(d, B_{\parallel}) = 4/(\pi\xi_0)/\sqrt{\sin\theta}$, that is shifted to higher critical values of the in-plane field (see Fig.1). [13] We also expect that because of the long-range (dipole) soliton interaction in the IC state, the usual [15] $1/|\ln(Q - Q_{CI})|$ rise in the soliton density will be replaced by a significantly slower $|Q - Q_{CC-IC}|^{1/2}$ increase inside the IC state. [13]

In contrast to the CC state, the charge imbalance m_z^z is a periodic function inside the IC state, even in the $d \rightarrow 0$ limit, oscillating with period a of the soliton lattice around the mean value of the charge imbalance $m_0^z(d, B_{\parallel})$.

The four QH phases that we have discussed are connected by novel continuous quantum phase transition discussed in Ref. [13]. We therefore expect and find a variety of universal experimental signatures near phase boundaries of Fig.1. As illustrated in Fig.2, some of many striking predictions is a strong d -dependent peak in the bilayer capacitance near the CP-CC phase boundary, as well as the development of spontaneous interlayer charge imbalance (proportional to m_z) inside the CC phase. We

expect, that these and other critical anomalies [13], as well as the dipolar stripe order of CC and IC phases, with period of order micron and tunable with d and B_{\parallel} , should be readily observable in experiments that we hope our work will stimulate.

In summary, we have computed d versus B_{\parallel} phase diagram for QH bilayers, and found that in addition to the previously studied planar commensurate and incommensurate phases (which at large d are unstable to a compressible “No-QHE” state), there exist interlayer charge imbalanced commensurate and incommensurate phases, in which pseudo-magnetization continuously cants out of the easy-xy-plane. We computed the charge imbalance, differential capacitance and single particle gap in these new phases, and suggested ways of accessing this physics experimentally.

This work was supported by the NSF MRSEC DMR-0080054 (MA), Oklahoma State Regents for Higher Education (MA), NSF DMR-9625111 (LR), the Sloan and Packard Foundations (LR), the Robert A. Welch Foundation (AHM), and by the NSF DMR-0115947 (AHM).

-
- [1] J. P. Eisenstein *et al.*, Phys. Rev. Lett. **68**, 1383 (1992).
 - [2] S. Q. Murphy *et al.*, Phys. Rev. Lett. **72**, 782 (1994).
 - [3] I. B. Spielman, *et al.*, Phys. Rev. Lett. **84**, 5808 (2000).
 - [4] I. B. Spielman, *et al.*, condmat/0012094.
 - [5] K. Muraki, *et al.*, Physica C, 2001.
 - [6] H. Fertig, Phys. Rev. B **40**, 1087 (1989).
 - [7] A. H. MacDonald, *et al.*, Phys. Rev. Lett. **65**, 775 (1990).
 - [8] X.-G. Wen, A. Zee, Phys. Rev. Lett. **69**, 1811 (1992); Z. Ezawa, A. Iwazaki, Phys. Rev. B **48**, 15189 (1993).
 - [9] K. Moon *et al.*, Phys. Rev. B **51**, 5138 (1995); K. Yang *et al.*, *ibid.* **54**, 11644 (1996).
 - [10] L. Balents, L. Radzihovsky, Phys. Rev. Lett. **86**, 1825 (2001); A. Stern *et al.*, *ibid.* 1829 (2001); M. Fogler, F. Wilczek *et al.*, *ibid.* 1833 (2001).
 - [11] A. H. MacDonald and E.H. Rezayi, Phys. Rev. B **42**, 3224 (1990); Daijiro Yoshioka and A.H. MacDonald, J. Phys. Soc. Jpn. **59**, 4211 (1990).
 - [12] T. Jungwirth and A.H. MacDonald, Phys. Rev. B **63**, 035305 (2001).
 - [13] L. Radzihovsky, cond-mat/0104128 and unpublished.
 - [14] A. Hubert and R. Schäfer, *Magnetic Domains* (Springer, Berlin, 1998).
 - [15] V. L. Pokrovsky, A. L. Talapov, Phys. Rev. Lett. **42**, 65 (1970); C. B. Hanna, *et al.*, Phys. Rev. B **63**, 125305 (2001).
 - [16] It has recently been proposed that states with exotic order parameters could occur in this regime. Y. B. Kim, *et al.*, cond-mat/0011459; M. Y. Veillette, *et al.*, cond-mat/0105118.
 - [17] The situation here is not different from ordinary ferromagnets (electrics), where for sufficiently long scales long-range dipolar interactions always dominate the exchange and lead to antiferro-magnetic (electric) domain structure.